Sphere–Rod Transition of Micelles of Tetradecyltrimethylammonium Halides in Aqueous Sodium Halide Solutions and Flexibility and Entanglement of Long Rodlike Micelles

Toyoko Imae* and Shoichi Ikeda

Department of Chemistry, Faculty of Science, Nagoya University, Nagoya 464, Japan
(Received: December 18, 1985; In Final Form: April 3, 1986)

Static light scattering from aqueous NaCl and NaBr solutions of tetradecyltrimethylammonium chloride (TTAC) and bromide (TTAB), respectively, has been measured at 25 °C. Spherical micelles are formed in water and in aqueous solutions with low salt concentrations. Rodlike micelles are formed above the threshold salt concentrations, which are 2.7 and 0.12 M for TTAC and TTAB, respectively, and their aggregation numbers markedly increase with an increase in salt concentration. With application of the wormlike chain model, the contour length and persistence length of long rodlike micelles of TTAB have been evaluated on the basis of simple geometrical assumptions. The same procedure has been applied for rodlike micelles of dodecyldimethylammonium chloride (DDAC) and bromide (DDAB) and cetyltrimethylammonium bromide (CTAB). Long rodlike micelles of these surfactants are flexible, but their persistence lengths for TTAB and CTAB, 51 and 47 nm, are slightly longer than those for DDAC and DDAB, 35 and 31 nm. The entanglement of long rodlike micelles at concentrations above overlap threshold micelle concentration is also discussed on the assumption that the blobs for the entangled network consisting of these micelles behave ideally. The radius of gyration of the blob of TTAB micelles is scaled for its molecular weight with the exponent, 0.54, the relation being in complete agreement with that with the exponent, 0.55, in the dilute region.

Introduction

In aqueous solutions many ionic surfactants can associate into rodlike micelles with increasing micelle concentration, if the salt concentration exceeds a certain threshold value.[1-4] The threshold salt concentration of the salt-induced sphere–rod transition is dependent on the counterion species, and the size of rodlike micelles grows with increasing salt concentration, in a different way depending on the counterion species.

Rodlike micelles are long and flexible when the salt concentration is high.[4] Some workers[4-9] have quantitatively discussed the flexibility of long rodlike micelles and estimated their persistence length in terms of the wormlike chain model. However, the methods by which the contour length of a rodlike micelle was evaluated from data of light scattering were different from one another: three groups[4,6,9] utilized the same data[1] of dodecyldimethylammonium chloride (DDAC) and obtained different persistence lengths, 82,[6] 45,[9] and 30 nm.[4]

At high micelle concentrations, rodlike micelles would overlap and entangle together. We have found that the overlap threshold concentration of rodlike micelles of cetyltrimethylammonium bromide (CTAB) decreases with increasing NaBr concentration.[4]

The solution properties of alkyltrimethylammonium bromide micelles in the semidilute region have recently been investigated by Candau et al.[10,11] They discussed the scaling laws for aqueous KBr solutions of CTAB above the overlap threshold concentration and supported a model of long and flexible micelles entangled together: the scaling law of the intensity of light scattering against the volume fraction of surfactant was obtained above the overlap threshold concentration, which excellently agreed with the theoretical prediction for polymer solutions in good solvents.[12]

In the present work we measure the static light scattering from aqueous NaCl and NaBr solutions of tetradecyltrimethylammonium chloride (TTAC) and bromide (TTAB), respectively, and determine the micelle molecular weight at different salt concentrations. We observe the salt-induced sphere–rod transition for both surfactants, TTAC and TTAB, and find that the rodlike micelles of TTAB become very long in aqueous solutions with high NaBr concentrations. For long rodlike micelles of TTAB the radius of gyration can be derived from the angular dependence of light scattering and it is related to the molecular weight. The flexibility of long rodlike micelles of TTAB is estimated on the basis of the wormlike chain model and is compared with that of homologous surfactants. We also evaluate the overlap threshold concentration of rodlike micelles of TTAB and discuss their entanglement.

Experimental Section

Materials. Samples of TTAC and TTAB purchased from Tokyo Kasei Kogyo Ltd., Tokyo, were recrystallized 3 times from ethanol–acetone, acetone, or acetone–ethyl acetate and dried for 8 h at 60 °C in vacuo. The purity of the recrystallized samples was checked by thermal decomposition gas chromatography, on which there was no appreciable peak arising from contaminant homologues. Commercial NaCl and NaBr were ignited for 1 h. Water was redistilled from alkaline $KMnO_4$ in a glass still.

Procedures. Light scattering measurements were carried out on a Union Giken automatic light scattering analyzer LS-601, equipped with an argon ion laser. The laser beam at 488 nm was vertically polarized, and the total scattered light in vertical and horizontal polarizations was collected by a photomultiplier.

The reduced intensity of light scattered at a scattering angle θ is given by

$$R_{\theta,U_v} = \phi_b \frac{\tilde{n}_0^2}{\tilde{n}_b^2} \frac{I_\theta}{I_0} \sin\theta \qquad (1)$$

where I_0 and I_θ are the measured intensities of incident and scattered light, respectively, and $\tilde{n}_0$ and $\tilde{n}_b$ are the refractive indices of the solvent and benzene, respectively. Hereafter, the suffix, U_v, for R_θ is omitted. The calibration constant of the apparatus for benzene, ϕ_b, was determined by using the value of the reduced intensity in the 90° direction of light scattered from benzene, 34.11 $\times 10^{-6}$ cm^{-1} at 488 nm.[4]

Solvents and solutions were clarified by filtration into a cylindrical cell through a membrane filter under pressure. The filtration was repeated 6 times. The membrane filters with pore sizes of 0.01–0.45 μm were cleaned by filtering redistilled water.

(1) Ikeda, S.; Ozeki, S.; Tsunoda, M. *J. Colloid Interface Sci.* **1980**, *73*, 27.
(2) Ozeki, S.; Ikeda, S. *J. Colloid Interface Sci.* **1982**, *87*, 424.
(3) Ozeki, S.; Ikeda, S. *Colloid Polym. Sci.* **1984**, *262*, 409.
(4) Imae, T.; Kamiya, R.; Ikeda, S. *J. Colloid Interface Sci.* **1985**, *108*, 215.
(5) Appell, J.; Porte, G.; Poggi, Y. *J. Colloid Interface Sci.* **1982**, *87*, 492.
(6) Flamberg, A.; Pecora, R. *J. Phys. Chem.* **1984**, *88*, 3026.
(7) Imae, T.; Ikeda, S. *Colloid Polym. Sci.* **1984**, *262*, 497.
(8) Imae, T.; Ikeda, S. *Colloid Polym. Sci.* **1985**, *263*, 756.
(9) Van De Sande, W.; Persoons, A. *J. Phys. Chem.* **1985**, *89*, 404.
(10) Candau, S. J.; Hirsch, E.; Zana, R. *J. Phys.* **1984**, *45*, 1263.
(11) Candau, S. J.; Hirsch, E.; Zana, R. *J. Colloid Interface Sci.* **1985**, *105*, 521.
(12) de Gennes, P.-G. *Scaling Concepts in Polymer Physics*; Cornell University Press: Ithaca, NY, and London, 1979.

0022-3654/86/2090-5216$01.50/0

TABLE I: Characteristics of TTAC Micelles in Aqueous NaCl Solutions at 25 °C

			spherical			rodlike	
C_s, M	$(\partial\tilde{n}/\partial c)_{C_s}$, cm^3 g^{-1}	10^2c_0, g cm^{-3}	$10^{-4}M$	m	10^3B, cm^3 g^{-1}	$10^{-4}M$	m
0	0.159	0.240	1.82	62.3	31.0		
0.5	0.159[a]	0.035	2.23	76.4	0.34		
1.0	0.159	0.010	2.23	76.4	0.31		
2.0	0.138	0.006	2.80	96.0	0.21		
2.5	0.133[a]	<0.001	3.23	111	0.23		
3.0	0.128	<0.001	2.99	102	~0	~4.00	~137
3.5	0.127					7.69	264
4.0	0.125					12.6	432

[a] Interpolated.

A cylindrical quartz cell 2 cm in diameter was set in a cell housing, which was filled with xylene and kept at 25 ± 0.1 °C.

Measurements of specific refractive index increment were carried out on a Union Giken differential refractometer RM-102A with light of 488 nm, which was isolated by a filter from the light of an iodine lamp. The cell housing was kept at 25 ± 0.1 °C, and the apparatus was calibrated by using aqueous solutions of NaCl.

Analysis. Light scattered from a dilute aqueous solution of micelles at the surfactant concentration, c (g cm^{-3}), can be described by

$$\frac{K(c - c_0)}{R_\theta - R_\theta^0} = \frac{1}{MP(\theta)} + 2B(c - c_0) \quad (2)$$

for a scattering angle θ, where M is the average molecular weight of micelles and B is the second virial coefficient. R_θ^0 is the reduced scattering intensity for the solution at the critical micelle concentration, c_0, and is substantially equal to the reduced scattering intensity of the solvent. K is the optical constant and is written as

$$K = \frac{4\pi^2\tilde{n}_0^2(\partial\tilde{n}/\partial c)_{C_s}^2}{N_A\lambda^4} \quad (3)$$

where $(\partial\tilde{n}/\partial c)_{C_s}$ is the specific refractive index increment of a solution at constant salt concentration, C_s (M), N_A is Avogadro's number, and λ is the wavelength of incident light.

The particle scattering factor, $P(\theta)$, at small scattering angles is given by

$$(1/P(\theta))_{\theta:\text{small}} = 1 + \tfrac{1}{3}R_G^2\mu^2 \quad (4a)$$

and

$$\mu = 4\pi\tilde{n}_0/\lambda \sin(\theta/2) \quad (4b)$$

irrespectively of micelle shape, where R_G is the average radius of gyration of micelles. If the scattering angle is extrapolated to zero or if there is no angular dependence of light scattering, the value of $P(\theta)$ is unity.

Results

Light Scattering from Aqueous NaCl Solutions of TTAC. The reduced scattering intensity at 90° scattering angle for aqueous NaCl solutions of TTAC is shown in Figure 1. It increases with increasing surfactant concentration beyond a certain concentration, assigned to the critical micelle concentration. The reduced scattering intensity is stronger and the critical micelle concentration is lower for solutions of higher NaCl concentrations. The dissymmetry in the 60° direction, $z_{60} = R_{60}/R_{120}$, was 1.00 ± 0.03 for all aqueous NaCl solutions of TTAC examined, and no angular dependence of reduced scattering intensity was observed.

The Debye plots at 90° scattering angle are shown in Figure 2. The Debye plots for aqueous solutions with NaCl concentrations up to 2.5 M linearly increase with an increase in micelle concentration, $c - c_0$. The micelle molecular weight and the second virial coefficient can be obtained from the intercept and the slope of the Debye plot, respectively, according to eq 2 with $P(\theta) = 1$. The micelle molecular weight ranges from 18 200 to 32 300, indicating the formation of spherical micelles with the aggregation number, $m = M/291.9$, from 62 to 111. Numerical values are summarized in Table I, together with values of the specific re-

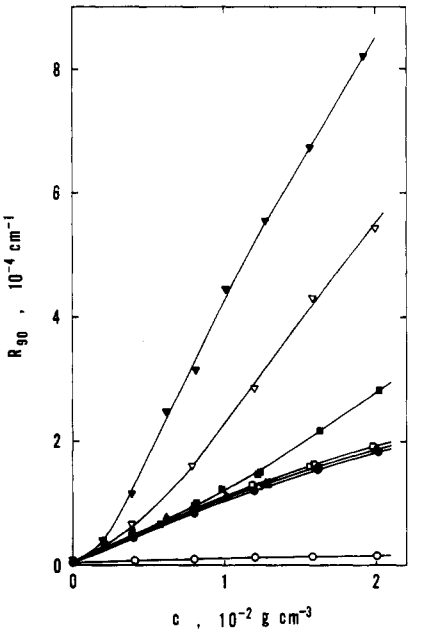

Figure 1. Plot of the reduced scattering intensity in the 90° direction vs. the surfactant concentration for aqueous NaCl solutions of TTAC. NaCl concentration (M): (○) 0; (●) 0.5; (△) 1.0; (▲) 2.0; (□) 2.5; (■) 3.0; (▽) 3.5; (▼) 4.0.

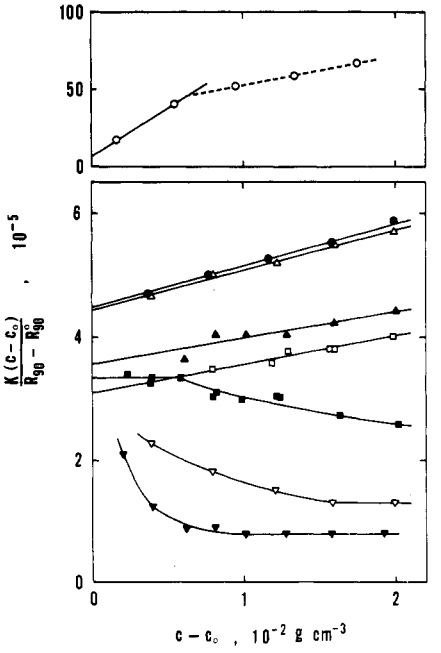

Figure 2. Debye plots of light scattering at the 90° scattering angle as a function of the micelle concentration for aqueous NaCl solutions of TTAC. The symbols represent the same NaCl concentrations as in Figure 1.

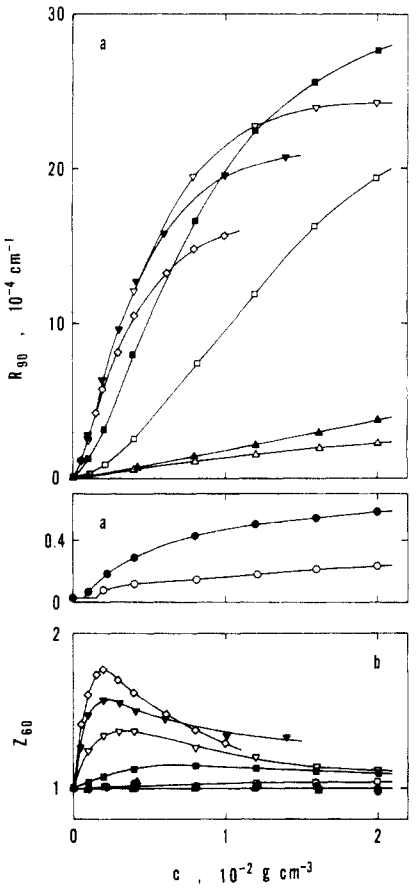

Figure 3. Plot of the reduced scattering intensity in the 90° direction (a) and the dissymmetry at 60° direction of scattered light (b) vs. the surfactant concentration for aqueous NaBr solutions of TTAB. NaBr concentration (M): (○) 0; (●) 0.01; (△) 0.10; (▲) 0.20; (□) 0.50; (■) 1.0; (▽) 2.0; (▼) 3.0; (◇) 4.0.

fractive index increment and the critical micelle concentration.

The Debye plot for TTAC micelles in water linearly increases with increasing micelle concentration, giving a second virial coefficient of 31.0×10^{-3} cm^3 g^{-1}, which suggests strong repulsion between micelles. However, the Debye plot deviates downward from a straight line when the micelle concentration exceeds 0.64×10^{-2} g cm^{-3}. Similar behavior was observed for CTAB micelles in water.[4,13] This phenomenon was interpreted as stronger binding of the counterion with the micelle above this concentration, thus weakening the intermicellar repulsion and reducing the value of the second virial coefficient.

The Debye plot for dilute solutions of TTAC in 3.0 M NaCl is horizontal and gives the value of molecular weight assignable to a spherical micelle. However, it decreases with an increase in micelle concentration above 0.58×10^{-2} g cm^{-3}. Above this micelle concentration, rodlike micelles would be formed. Accordingly, TTAC undergoes two-step micellization in 3.0 M NaCl. Similar two-step micellization was already reported for aqueous NaBr solutions of dodecyltrimethylammonium bromide (DTAB).[2]

The Debye plots for 3.5 and 4.0 M NaCl solutions of TTAC decrease with an increase in micelle concentration and approach constant values at high micelle concentrations. The constant value at high micelle concentrations can be identified with the reciprocal molecular weight of rodlike micelles, because the second virial coefficient is negligible for micelles owing to their large molecular weight[4] and the strong shielding of electrostatic repulsion in the presence of concentrated NaCl. Numerical values of micelle molecular weight and aggregation number are given in Table I. Thus in 3.5 and 4.0 M NaCl spherical micelles are formed at the critical micelle concentration, but they associate together to form rodlike micelles as the micelle concentration is increased.

Light Scattering from Aqueous NaBr Solutions of TTAB. The reduced scattering intensity in the 90° direction for aqueous NaBr solutions of TTAB is shown in Figure 3a. The reduced scattering

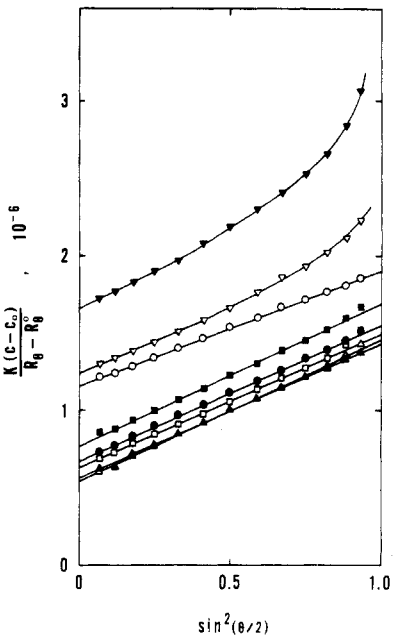

Figure 4. Reciprocal angular envelope of light scattering for 3.0 M NaBr solutions of TTAB. Micelle concentration (10^{-2} g cm^{-3}): (○) 0.052; (●) 0.096; (△) 0.196; (▲) 0.299; (□) 0.413; (■) 0.599; (▽) 1.005; (▼) 1.402.

intensity increases with increasing surfactant concentration above the critical micelle concentration, and the curve has a downward curvature when the NaBr concentration is lower than 0.20 M. For 0.20–4.0 M NaBr solutions, the reduced intensity increases with an upward curvature at low surfactant concentrations and with a downward curvature at high surfactant concentrations. The reduced intensity generally increases with increasing NaBr concentration. However, at high surfactant concentrations it tends to decrease with an increase in NaBr concentration above 1.0 M.

The dissymmetry at 60° scattering angle for 0–0.20 M NaBr solutions has a value of unity within experimental errors, while for 0.50 M NaBr solution it increases with an increase in surfactant concentration and becomes constant at high surfactant concentrations. This can be seen in Figure 3b. At high NaBr concentrations, the dissymmetry increases with increasing surfactant concentration, but it reaches a maximum and then decreases with a further increase in surfactant concentration. A maximum appears at a lower surfactant concentration for a higher NaBr concentration.

The light scattering for 0.50–4.0 M NaBr solutions of TTAB depends on the scattering angle. The reciprocal angular envelope of light scattering linearly increases with increasing $\sin^2(\theta/2)$ for all NaBr concentrations, except for some 3.0 M NaBr solutions, as seen in Figure 4. The extrapolation of the straight line to zero scattering angle gives light scattering free from internal interference. The reciprocal angular envelope of light scattering for 3.0 M NaBr solutions having TTAB concentrations 1.01×10^{-2} and 1.40×10^{-2} g cm^{-3} is linear at low scattering angles but appreciably increases at high angles.

Figure 5 shows the Debye plots in the 0° direction for 0.50–4.0 M NaBr solutions, together with those in the 90° direction for 0–0.20 M NaBr solutions. The Debye plot for micellar solutions of TTAB in water linearly increases with increasing micelle concentration but deviates from a straight line at high micelle concentrations, as observed for micellar solutions of TTAC and CTAB in water. The deviation from the initial straight line takes place above 0.77×10^{-2} g cm^{-3}, which is higher than 0.64×10^{-2} g cm^{-3} for TTAC and $(0.3–0.4) \times 10^{-2}$ g cm^{-3} for CTAB.[4,13]

The molecular weight of spherical micelles of TTAB in water and the second virial coefficient of their solutions can be obtained from the intercept and slope of the initial straight line. The molecular weight of spherical micelles in water is 23 800 and its

(13) Ekwall, P.; Mandell, L.; Solyom, P. *J. Colloid Interface Sci.* **1971**, *35*, 519.

TABLE II: Characteristics of TTAB Micelles in Aqueous NaBr Solutions at 25 °C

			spherical			rodlike			
C_s, M	$(\partial\bar{n}/\partial c)_{C_s}$, cm^3 g^{-1}	10^2c_0, g cm^{-3}	$10^{-4}M$	m	10^3B, cm^3 g^{-1}	10^2c,[a] g cm^{-3}	$10^{-4}M$	m	R_G, nm
0	0.153	0.130	2.38	70.8	18.1				
0.01	0.153	0.060	2.53	75.3	3.41				
0.10	0.153	0.015	3.35	100	0.34				
0.20	0.153	0.008	3.41	101	~0				
0.50	0.153					1.59	21.9	650	15.2
1.0	0.153					0.805	48.5	1440	28.1
2.0	0.132					0.297	124	3690	46.4
3.0	0.121					0.196	185	5510	63.6
4.0	0.095_5					0.195	333	9910	77.8

[a] The molecular weight and radius of gyration of rodlike micelles are obtained at given surfactant concentrations.

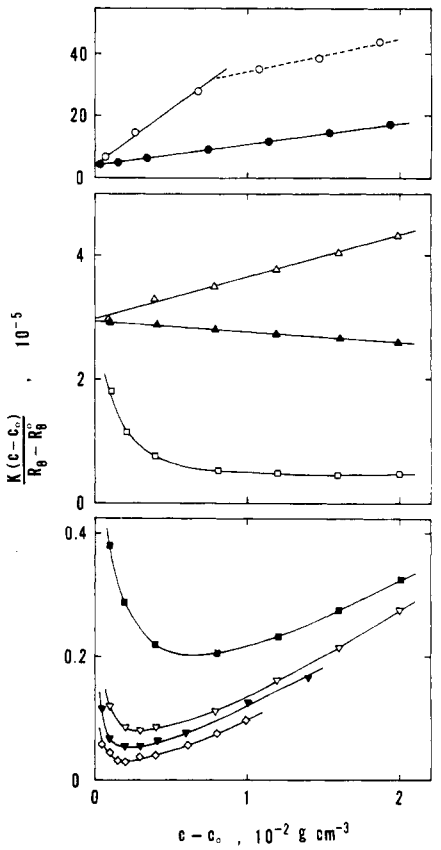

Figure 5. Debye plots of light scattering at the scattering angle θ as a function of the micelle concentration for aqueous NaBr solutions of TTAB. θ = 90° for 0–0.20 M NaBr solutions; θ = 0° for 0.50–4.0 M NaBr solutions. The symbols represent the same NaBr concentrations as in Figure 3.

aggregation number, $m = M/336.4$, is 71. The second virial coefficient, 18.1 × 10^{-3} cm^3 g^{-1}, for TTAB in water is of the same order of magnitude as those of TTAC and CTAB[4] in water, but it is larger than those for dodecyltrimethylammonium chloride (DTAC)[14] and DTAB[15] in water. Thus the spherical micelles of TTAC, TTAB, and CTAB interact with one another more strongly than those of DTAC and DTAB. This is caused by differences in the excluded volume effect and the electrostatic repulsion of micelles. It is noted that Trap and Hermans[15] reported a micelle molecular weight of 30 800 and a second virial coefficient of 18.6 × 10^{-3} cm^3 g^{-1} for aqueous solutions of TTAB.

For 0.01 and 0.10 M NaBr solutions of TTAB, linear relations hold for the Debye plot, and the characteristics of spherical micelles can be readily obtained. The Debye plot for 0.20 M NaBr solution is a straight line, having a weakly negative slope, and this can be interpreted as the gradual formation of rodlike micelles with an increase in micelle concentration.

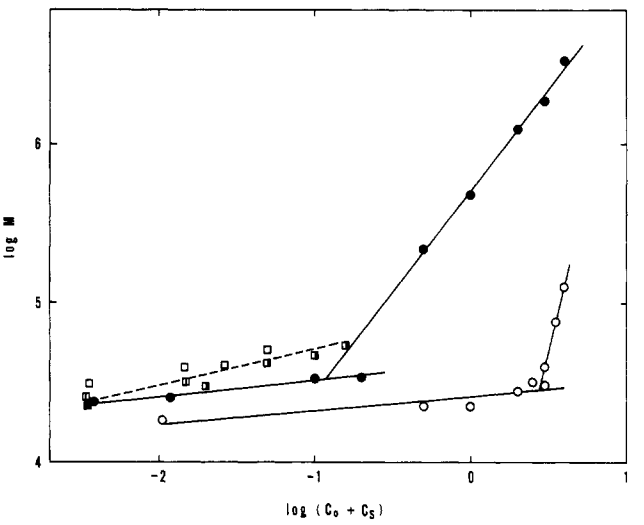

Figure 6. Double logarithmic plot of M vs. (C_0 + C_s) for TTAC and TTAB micelles. (○) TTAC in aqueous NaCl solutions at 25 °C; (●) TTAB in aqueous NaBr solutions at 25 °C; (□) TTAB in aqueous KBr solutions at 30 °C (ref 15); (■) TTAB in water at 25 °C (ref 17); (▣) TTAB in aqueous KBr solutions at 25 °C (ref 18); (◨) TTAB in aqueous KBr solutions at 25 °C (ref 19).

The Debye plot for 0.50 M NaBr solutions of TTAB initially decreases strongly with increasing micelle concentration and levels off at high micelle concentrations. For 1.0–4.0 M NaBr solutions the Debye plots decrease sharply, pass a minimum, and increase with increasing micelle concentration. While the initial decrease in the Debye plots indicates the transition from spherical to rodlike micelles depending on the surfactant concentration, the constant or minimum values of the Debye plots can be assigned to the reciprocal molecular weights of rodlike micelles, neglecting the contribution of the second virial coefficient there. Correspondingly, the slope of the straight line for reciprocal angular envelope of light scattering at these concentrations gives the value of the radius of gyration of rodlike micelles. Table II gives the characteristics of TTAB micelles in aqueous NaBr solutions, including values of the specific refractive index increment and the critical micelle concentration. For 1.0–4.0 M NaBr solutions, the strong increase in the Debye plots above a minimum value with increasing micelle concentration originates from the overlap of rodlike micelles. This is discussed below.

Discussion

Sphere–Rod Transition of TTAC and TTAB Micelles. The micelle molecular weights of TTAC and TTAB in aqueous NaCl and NaBr solutions, respectively, are plotted against the ionic strength or the molar concentration of counterion on a double logarithmic scale in Figure 6. Two linear relations hold for TTAC and TTAB micelles, each corresponding to spherical and rodlike micelles. These linear relations can be represented by

$$\log M = 0.09 \log (C_0 + C_s) + 4.42 \qquad C_s < 3.0 \text{ M} \qquad (5a)$$

$$\log M = 3.99 \log (C_0 + C_s) + 2.70 \qquad C_s \geq 2.7 \text{ M} \qquad (5b)$$

(14) Ozeki, S.; Ikeda, S. *Bull. Chem. Soc. Jpn.* **1981**, *54*, 552.
(15) Trap, H. J. L.; Hermans, J. J. *Proc. Ned. Akad. Wet., Ser. B: Phys. Sci.* **1955**, *58*, 97.

for TTAC micelles in aqueous NaCl solutions and by

$$\log M = 0.11 \log (C_0 + C_s) + 4.62 \qquad C_s < 0.20 \text{ M} \qquad (6a)$$

$$\log M = 1.28 \log (C_0 + C_s) + 5.71 \qquad C_s \geq 0.12 \text{ M} \qquad (6b)$$

for TTAB micelles in aqueous NaBr solutions.

The slope of the straight line for spherical micelles is almost equal for TTAC and TTAB, and it is also identical with those for DTAC,[14] DTAB,[2] and CTAB.[4] The slope of the line for rodlike micelles of TTAC is 3 times as large as that of TTAB. For alkyltrimethylammonium bromide it increases from 1.11 for DTAB[2] to 2.07 for CTAB.[4]

The threshold NaCl concentration for the sphere–rod transition of TTAC micelles is 2.7 M, and it corresponds to the micelle molecular weight 28 100 and the aggregation number 96. The threshold NaBr concentration for the sphere–rod transition of TTAB micelles, 0.12 M, is lower than that for TTAC micelles, and it is at the micelle molecular weight 32 800 and the aggregation number 98. The sphere–rod transition of micelles of tetradecyltrimethylammonium halide occurs around the aggregation number 97, independent of counterion species. This result cannot be generalized, however, since micelles of dodecyldimethylammonium halide undergo the sphere–rod transition at aggregation numbers 108 and 95 for chloride and bromide derivatives, respectively.[1,3]

Our value of the micelle molecular weight of TTAB in water is in agreement with those obtained by Venable et al.[16] and by Guveli et al.[17] However, the micelle molecular weight of TTAB in 0.05 M NaBr measured at room temperature by Venable et al. is higher than that estimated from eq 6a.

Debye[18] and Drifford et al.[19] measured the micelle molecular weights of TTAB in aqueous KBr solutions, and Trap and Hermans[15] measured them at 30 °C. Their values are also plotted in Figure 6, and they give a straight line represented by

$$\log M = 0.23 \log (C_0 + C_s) + 4.94 \qquad C_s < 0.16 \text{ M} \quad (7)$$

The slope, 0.23, for spherical micelles in aqueous KBr solutions is larger than that in aqueous NaBr solutions. This indicates the effect of co-ion species on the size of spherical micelles. Such an effect of co-ion species was found for micelles of CTAB[4] and sodium dodecyl sulfate.[20–22]

Nicoli and co-workers[23,24] measured dynamic light scattering from aqueous solutions of TTAB at different NaBr concentrations and at different temperatures, and they found that the dependence of diffusion coefficient on the NaBr concentration changes from positive to negative between 0.1 and 0.2 M NaBr at 25 °C. This range of NaBr concentration corresponds to the threshold NaBr concentration for the sphere–rod transition.

Flexibility of Long Rodlike Micelles. Figure 7 shows the double logarithmic plot of radius of gyration and molecular weight for rodlike micelles of TTAB. Data for rodlike micelles of DDAC,[1] dodecyldimethylammonium bromide (DDAB),[3] and CTAB[4] are also included in Figure 7. The relation, $R_G \sim M^{0.55}$, holds for TTAB and CTAB. Since the exponent, 0.55, is in the range of 0.5 for the ideal random coil and 0.6 for the real random coil in a good solvent[12] rather than unity for a rigid and thin rod,[25] rodlike micelles of TTAB and CTAB must be substantially flexible. On the other hand, the double logarithmic plots for rodlike micelles of DDAC and DDAB tend to obey the relation $R_G \sim M$ at lower

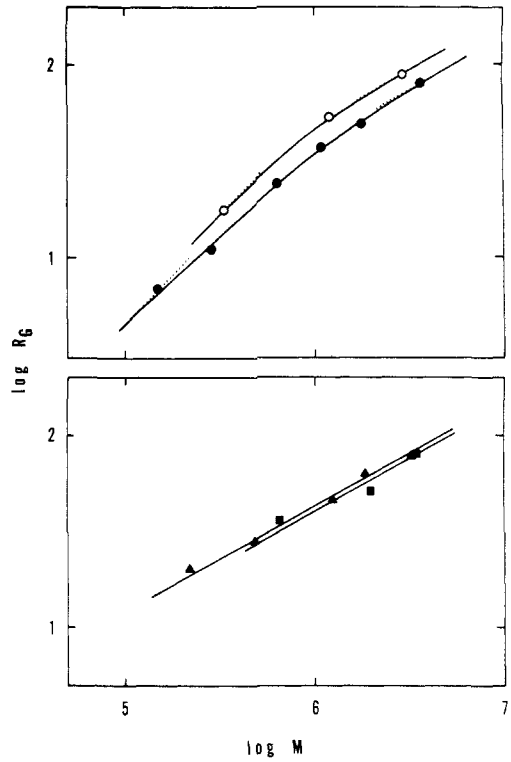

Figure 7. Double logarithmic plot of R_G vs. M for rodlike micelles of alkyldi- and alkyltrimethylammonium halides. (○) DDAC; (●) DDAB; (▲) TTAB; (■) CTAB. The dotted line at lower micelle molecular weights for DDAC and DDAB represents a theoretical line with a slope of unity and that at higher micelle molecular weights is a theoretical line with a slope of 0.5.

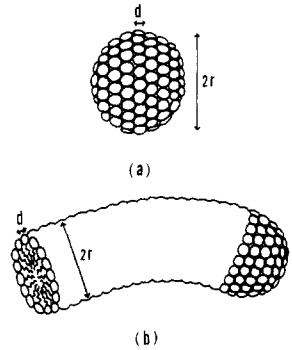

Figure 8. Schematic representation of a spherical micelle (a) and a portion of a rodlike micelle (b).

micelle molecular weights, but they follow the relation $R_G \sim M^{0.5}$ or $R_G \sim M^{0.6}$ at higher micelle molecular weights. Rodlike micelles of DDAC and DDAB are fairly flexible if they are sufficiently long.

If a long rodlike micelle is represented by a wormlike chain, its flexibility can be estimated on the basis of the theory of Kratky and Porod,[26] for which the contour length, L_c, and the persistence length, a, serve as characteristic parameters. Then the mean square radius of gyration, $\langle R_G^2 \rangle_0$, and the mean square end-to-end distance, $\langle r^2 \rangle_0$, for wormlike chains are expressed by[26,27]

$$\frac{\langle R_G^2 \rangle_0}{a^2} = \frac{L_c}{3a} - 1 + \frac{2a}{L_c}\left[1 - \frac{a}{L_c}(1 - e^{-L_c/a})\right] \qquad (8)$$

and

$$\frac{\langle r^2 \rangle_0}{2a^2} = \frac{L_c}{a} - 1 + e^{-L_c/a} \qquad (9)$$

(16) Venable, R. L.; Nauman, R. V. *J. Phys. Chem.* **1964**, *68*, 3498.
(17) Güveli, D. E.; Kayes, J. B.; Davis, S. S. *J. Colloid Interface Sci.* **1979**, *72*, 130.
(18) Debye, P. *Ann. N.Y. Acad. Sci.* **1949**, *51*, 575.
(19) Drifford, M.; Belloni, L.; Dalbiez, J. P.; Chattopadhyay, A. K. *J. Colloid Interface Sci.* **1985**, *105*, 587.
(20) Huisman, H. F. *Proc. Ned. Akad. Wet., Ser. B: Phys. Sci.* **1964**, *67*, 388.
(21) Ikeda, S.; Hayashi, S.; Imae, T. *J. Phys. Chem.* **1981**, *85*, 106.
(22) Doughty, D. A. *J. Phys. Chem.* **1983**, *87*, 5286.
(23) Briggs, J.; Dorshow, R. B.; Bunton, C. A.; Nicoli, D. F. *J. Chem. Phys.* **1982**, *76*, 775.
(24) Dorshow, R. B.; Bunton, C. A.; Nicoli, D. F. *J. Phys. Chem.* **1983**, *87*, 1409.
(25) Geiduschek, E. P.; Holtzer, A. *Adv. Biol. Med. Phys.* **1958**, *6*, 431.
(26) Kratky, O.; Porod, G. *Recl. Trav. Chim. Pays-Bas* **1949**, *68*, 1106.
(27) Benoit, H.; Doty, P. *J. Phys. Chem.* **1953**, *57*, 958.

TABLE III: Micelle Parameters of Alkyltrimethylammonium Halides

	$\bar{V}$, cm^3 mol^{-1}	ref	m_s	ref	r, nm	A_1, nm^2/molecule	d, nm	m_d	M_L, nm^{-1}
DAC	241.0	28 (23 °C)	80.4	35 (30 °C)	1.9_7	0.61	0.78	16	4510
DDAC	272.3	29 (25 °C)	55.6	1 (25 °C)	1.8_2	0.73	0.85	13	3890
DTAC	290.3	30 (25 °C)	43.6	14 (25 °C)	1.7_1	0.85	(0.92	12	3360)[a]
TTAC	319.3	28 (23 °C)	62.3	(25 °C)	1.9_9	0.80	0.89	14	4570
CTAC	355.2	31 (27 °C)	80 84	36 (25 °C) 31 (27 °C)	2.2_6	0.78	0.88	16	5800
DDAB	282.0	32 (25 °C)	77.1	3 (25 °C)	2.0_5	0.69	0.83	16	5500
DTAB	298.4	30 (25 °C)	53.0	30 (25 °C)	1.8_4	0.81	0.90	13	4420
TTAB	328.0 331.2	33 (25 °C) 34 (25 °C)	70.8	(25 °C)	2.1_0	0.78	0.89	15	5670
CTAB	365.4 363.0 364.0	34 (25 °C) 31 (27 °C) 33 (28 °C)	91	4 (35 °C)	2.3_6	0.77	0.88	17	7030

[a] DTAC does not form rodlike micelles in aqueous NaCl solutions.[14]

TABLE IV: Contour Length, Flexibility Parameters, and Overlap Threshold Concentration of Rodlike Micelles

	C_s, M	10^2c,[a] g cm^{-3}	$10^{-4}M$	R_G, nm	L_c, nm	a, nm	$L_c/2a$	$\langle r^2\rangle_0^{1/2}$, nm	10^2c^*, g cm^{-3}	C^*, M
DDAC in	2.0	0.78	33.3	17.4	85.7	18.1	2.3	49.6	2.51	0.100
NaCl (25 °C)[1]	3.0	0.20	120	51.5	309	35.4	4.4	139	0.35	0.014
	4.0	0.24	294	88.4	757	35.5	10.6	226	0.17	0.0068
DDAB in	0.2	1.4	15.0	6.9	27.1	19.5	0.69	22.0	18.10	0.615
NaBr (25 °C)[3]	0.3	0.95	29.0	11.0	52.4	12.8	2.0	32.0	8.64	0.293
	0.5	0.50	64.3	24.0	116	26.7	2.2	69.3	1.84	0.063
	0.7	0.40	109	37.1	197	32.7	3.0	104	0.85	0.029
	1.0	0.35	176	49.1	318	29.6	5.4	131	0.59	0.020
	1.5	0.35	357	79.7	646	34.5	9.4	205	0.28	0.0095
TTAB in	0.5	1.59	21.9	15.2	38.6	>3000	<0.01		2.48	0.074
NaBr (25 °C)	1.0	0.81	48.5	28.1	85.6	>5000	<0.01		0.87	0.026
	2.0	0.30	124	46.4	219	55.5	2.0	135	0.49	0.015
	3.0	0.20	185	63.6	327	60.3	2.7	179	0.29	0.0085
	4.0	0.20	333	77.8	588	37.0	8.0	202	0.28	0.0083
CTAB in	0.2	0.49	66.2	36.2	94.2	>3500	<0.01		0.55	0.015
NaBr (35 °C)[4]	0.3	0.29	197	51.0	280	41.6	3.4	141	0.59	0.016
	0.5	0.17	347	80.2	494	52.6	4.7	215	0.27	0.007

[a] The molecular weight and radius of gyration are obtained at given surfactant concentration, which are nearly equal to micelle concentrations.

where the subscript 0 means that the excluded volume effect is not included.

In order to evaluate the contour length for a rodlike micelle, we first postulate that each surfactant ion in a micelle occupies an identical area of cross-section, irrespective of whether it is in a spherical micelle in water or in a rodlike micelle in aqueous salt solutions. Furthermore, we assume that the spherical micelle in water is a sphere and the rodlike micelle has a circular cross-section with a radius equal to that of the sphere.

If a spherical micelle in water is a sphere with a radius r, as drawn in Figure 8, and has an aggregation number m_s, then its volume, V, and surface area, A, are given by

$$V = (4/3)\pi r^3 = \bar{V}m_s/N_A \quad (10a)$$

$$A = 4\pi r^2 = A_1 m_s \quad (10b)$$

respectively, where $\bar{V}$ is the partial molar volume of surfactant in spherical micelles in water and A_1 is the area per surfactant molecule or ion on the micelle surface.

A rodlike micelle is regarded as having a circular cross-section with a radius equal to r, on which the surface area per surfactant molecule or ion is equal to A_1. If the rodlike micelle consists of a stack of disklike layers, each having a thickness

$$d = (A_1)^{1/2} \quad (11)$$

as shown in Figure 8, the number of surfactant molecules or ions in a layer, m_d, is equal to

$$m_d = 2\pi r/d \quad (12)$$

Then the molecular weight per unit length of a micelle, M_L, is given by

$$M_L = M_1 m_d/d \quad (13)$$

where M_1 is the molecular weight of surfactant monomer and the contour length of a micelle can be calculated by

$$L_c = (M - M_1 m_s)/M_L + 2r \approx M/M_L \quad (14)$$

The values of $\bar{V}$ and m_s observed for spherical micelles in water are given in Table III, which includes data for TTAC and TTAB, together with those for dodecylammonium chloride (DAC), DDAC, DDAB, and homologous alkyltrimethylammonium halides.[1,3,4,14,28-36] The values of various micelle parameters calculated according to eq 10–13 are also summarized in Table III.

The contour length, persistence length, and end-to-end distance of rodlike micelles of TTAB can be evaluated by eq 8, 9, and 14 by using the observed values of micelle molecular weight and radius of gyration and assuming $\langle R_G^2\rangle_0 \approx R_G^2$. The numerical values are presented in Table IV, in which values of the number of Kuhn's segments, $L_c/2a$, are also given. When the contour length is longer than 200 nm, the persistence length of TTAB micelles is 37–60 nm. It is clear that long rodlike micelles of TTAB are generally flexible and behave like wormlike chains. For short rodlike micelles of TTAB in 0.50 and 1.0 M NaBr, however, their contour length is shorter than the length of Kuhn's segments,

(28) Mukerjee, P. *J. Phys. Chem.* **1962**, *66*, 1733.
(29) Ozeki, S.; Ikeda, S. *J. Colloid Interface Sci.* **1980**, *77*, 219.
(30) Imae, T.; Abe, A.; Taguchi, Y.; Ikeda, S. *J. Colloid Interface Sci.* **1986**, *109*, 567.
(31) Husson, F. R.; Luzzati, V. *J. Phys. Chem.* **1964**, *68*, 3504.
(32) Okuda, H.; Ozeki, S.; Ikeda, S. *Bull. Chem. Soc. Jpn.* **1984**, *57*, 1321.
(33) Güveli, D. E.; Keyes, J. B.; David, S. S. *J. Colloid Interface Sci.* **1981**, *82*, 307.
(34) Corkill, J. M.; Goodman, J. F.; Walker, T. *Trans. Faraday Soc.* **1967**, *63*, 768.
(35) Kushner, L. M.; Hubbard, W. D.; Parker, R. A. *J. Res. Natl. Bur. Stand.* **1957**, *59*, 113.
(36) Roelants, E.; Gelade, E.; Van der Auweraer, M.; Croonen, Y.; De Schryver, F. C. *J. Colloid Interface Sci.* **1983**, *96*, 288.

TABLE V: Characteristics of Entangled Rodlike Micelles of TTAB at 25 °C

C_s, M	10^2c, g cm^{-3}	c/c^*	$10^{-4}M_\xi$	ξ_G, nm	$10^{-23}N_\xi$	$L_{c,\xi}$, nm	a_ξ, nm	$L_{c,\xi}/2a_\xi$	ξ_r, nm
1.0	1.206	1.39	42.9	26.6	16.9	75.7			
	1.600	1.85	36.4	24.5	26.5	64.2			
	2.008	2.32	30.7	22.6	39.4	54.2			
2.0	0.792	1.62	89.7	41.2	5.32	158	143	0.55	133
	1.196	2.43	62.0	32.9	11.6	109			
	1.599	3.25	46.5	28.2	20.7	82.0			
	1.996	4.06	36.4	24.5	33.0	64.2			
3.0	0.299	1.05	179	60.9	1.01	316	56.6	2.8	171
	0.413	1.44	157	56.5	1.58	277	60.6	2.3	162
	0.599	2.10	131	53.6	2.75	231	89.1	2.2	162
	1.005	3.52	80.3	40.2	7.54	142	819	0.86	138
	1.402	4.90	60.4	37.2	14.0	107			
4.0	0.297	1.06	269	68.5	0.665	474	37.0	6.4	180
	0.400	1.43	243	65.0	0.991	429	37.9	5.7	172
	0.609	2.17	174	54.4	2.11	307	42.0	3.7	149
	0.797	2.84	132	46.5	3.64	233	47.1	2.5	132
	0.997	3.55	103	39.8	5.83	182	53.0	1.7	117

$2a$, and the micelles behave like nearly rigid rods. Rodlike micelles of TTAC are too short to be treated as wormlike chains and can be regarded as stiff rods.

In a previous paper[4] we evaluated the flexibility parameters of rodlike micelles of DDAC, DDAB, and CTAB by using different values for micelle parameters. We recalculate them by using revised values for micelle parameters, as given in Table IV. The rodlike micelles of CTAB in 0.20 M NaBr are too short to estimate their flexibility parameters. The contour lengths of rodlike micelles of DDAC in 2.0 M NaCl and of DDAB in 0.20 and 0.30 M NaBr are comparable with or shorter than the lengths of Kuhn's segments if the latter are evaluated for long rodlike micelles of the same surfactant. Then the evaluated numerical values of persistence length will be meaningless. These rodlike micelles would behave as stiff rods, as is also imagined from the relation between R_G and M in Figure 7.

As is seen in Table IV, the persistence lengths of long rodlike micelles, except for cases above mentioned, can be considered as approximately constant, independent of the salt concentration. It is, on the average, 35 ± 0, 31 ± 2, 51 ± 7, and 47 ± 6 nm for DDAC, DDAB, TTAB, and CTAB, respectively. Then the number of Kuhn's segments is 2–10 and the end-to-end distance is $^1/_2$ to $^1/_3$ of the contour length. Consequently it would be permissible to consider that the flexibility is independent of the contour length of rodlike micelles if the contour length is longer than the length of Kuhn's segments. This is plausible, as the surface charge density on a micelle depends on the counterion binding on its surface; if the salt concentration is high, the counterion binding should be independent of salt concentration, although it is affected by the surfactant ion species and the added salt species. It may be stated that the threshold values of the molecular weight and the contour length between stiff and flexible rodlike micelles are about 10^6 and 100 nm, respectively.

Table III shows the effects of size of head group, chain length, and counterion species on micelle parameters. The substitution of a CH_3 group for a H atom on the N atom of dodecylammonium ion increases $\bar{V}$, A_1, and d and decreases m_s, r, m_d, and M_L. The addition of a CH_2 group on the alkyl chain of alkyltrimethylammonium ion and the change of counterion species from Cl^- to Br^- both increase $\bar{V}$, m_s, r, m_d, and M_L but decrease A_1 and d.

When we refer to these micelle parameters, we may have the following criteria for the factors determining the persistence length of long rodlike micelles. The size of the head group determines the packing of surfactant molecules in a rodlike micelle, the chain length alters the radius of its cross-section, and the counterion species defines its surface charge density. When the packing of surfactant molecules is looser, the cross-sectional radius is smaller, the surface charge density is lower, and the rodlike micelle is more flexible. A rise of temperature may also induce flexibility on the rodlike micelle. The persistence length of long rodlike micelles of ionic surfactant should be determined by the balance between these factors.

We have previously derived the value of M_L of 12000 for rodlike micelles of dimethyloleylamine oxide (DOAO) unequivocally from an analysis of experimental data[7] and evaluated their flexibility parameters in both uncharged and weakly charged states.[7,8] Their persistence lengths were found to be longer than 107 nm, indicating their considerable stiffness. This is because rodlike micelles of DOAO have a larger radius of cross-section (~30 nm) and stronger hydration on it, in spite of a lower or zero surface charge density.

The persistence length of rodlike micelles was first estimated by Appell et al.[5] as 20 nm for micelles of cetylpyridinium bromide in aqueous NaBr solutions. However, they postulated polydispersity of rodlike micelles based on a quasiisodesmic association mechanism. Flamberg and Pecora[6] reported the persistence length of 82 nm for rodlike micelles of DDAC. They calculated the contour length, using Tanford's relation[37] for the volume of a micelle core associated with the aggregation number. In a previous work[4] we pointed out that their procedure of evaluating the contour length does not necessarily lead to a reasonable value of flexible rodlike micelles of CTAB. Van De Sande and Persoons[9] reported the persistence length, 45 nm, for micelles of both DDAC and DDAB, which is closer to ours. They estimated the contour length by using the assumed values of partial molar volume and cross-sectional radius for rodlike micelles.

Entanglement of Long Rodlike Micelles. When the concentration of rodlike micelles exceeds a certain threshold concentration, rodlike micelles may overlap together. The overlap threshold concentration, c^* (g cm^{-3}) or C^* (M), is preferably estimated by

$$c^* = M/[(4/3)\pi R_G^3 N_A] \quad (15)$$

or

$$C^* = 1000c^*/M \quad (16)$$

although some workers[6,9] discussed the entanglement of rodlike micelles by using the theory for long and rigid thin rods by Doi and Edwards.[38] The c^* and C^* values calculated for rodlike micelles of TTAB are shown in Table IV. It may be remarked that these concentrations are higher by only (0.1–0.2) × 10^{-2} g cm^{-3} than the micelle concentrations for the maximum dissymmetry or for the minimum of the Debye plot, these latter two extremes being nearly equal to each other.

The c^* and C^* values for homologous surfactants at given salt concentrations are also listed in Table IV. The overlap threshold concentrations are higher than the concentrations at which the molecular weight and radius of gyration of rodlike micelles were observed, except for the 4.0 M NaCl solution of DDAC and the

(37) Tanford, C. *The Hydrophobic Effect: Formation of Micelles and Biological Membranes*, 2nd ed.; Wiley-Interscience: New York, 1980.
(38) Doi, M.; Edwards, S. F. *J. Chem. Soc., Faraday Trans. 2* **1978**, *74*, 560.

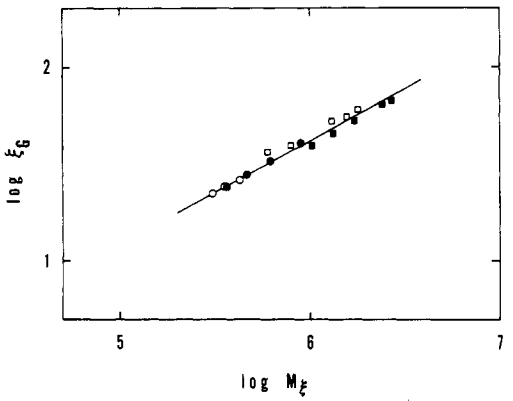

Figure 9. Double logarithmic plot of ξ_G vs. M_ξ for entangled rodlike micelles of TTAB. NaBr concentration (M): (○) 1.0; (●) 2.0; (□) 3.0; (■) 4.0.

1.5 M NaBr solution of DDAB. They decrease with increasing salt concentration.

Candau et al.[10,11] measured light scattering from semidilute solutions of DTAB, TTAB, and CTAB in 0.1 and 0.25 M KBr and found the overlap threshold concentration to be 0.05 M for 0.1 M KBr solutions of CTAB. They defined it as the concentration where the maximum scattering intensity or the minimum diffusion coefficient was observed.

When the micelle (or surfactant) concentration exceeds the overlap threshold concentration, rodlike micelles entangle together to form a network with an average mesh size ξ, called the correlation length.[12] If M_ξ is the molecular weight of a blob that is a unit of mesh and N_ξ is the number of blobs in a unit volume, then

$$c \approx c - c_0 = M_\xi N_\xi / N_A \qquad (17)$$

The light scattered from an aqueous solution of micelles in the semidilute region can be expressed by

$$R_\theta - R_\theta^0 = K(c - c_0)M_\xi[1 - (1/3)\xi_G^2\mu^2]S_\xi(\theta) \qquad (18)$$

for a scattering angle θ, where ξ_G is the radius of gyration of a blob and $S_\xi(\theta)$ is the structure factor of blobs. If blobs are independent of one another, that is, $S_\xi(\theta) = 1$, the values of M_ξ and ξ_G for rodlike micelles of TTAB can be obtained from light scattering data for semidilute solutions above the overlap threshold concentration. Numerical values of blob parameters are summarized in Table V. Values of M_ξ and ξ_G decrease but the value of N_ξ increases with an increase of micelle concentration.

Figure 9 shows the double logarithmic plot of ξ_G vs. M_ξ for entangled rodlike micelles of TTAB. The scaling law, $\xi_G \sim M_\xi^{0.54}$, holds for the semidilute solutions, independently of the NaBr concentration. This relation is consistent with the scaling law $R_G \sim M^{0.55}$ found in dilute micellar solutions with different NaBr concentrations. We may conclude that the characteristics of rodlike micelles are not perturbed by their entanglement.

In Table V, values of the contour length, $L_{c,\xi}$, the persistence length, a_ξ, the number of Kuhn's segments, $L_{c,\xi}/2a_\xi$, and the end-to-end distance, ξ_r, associated with a blob are included with the value of the ratio c/c^*. With increasing ratio c/c^*, the contour length, the number of Kuhn's segments, and the end-to-end distance decrease, while the persistence length increases, indicating that the blobs become smaller.

Acknowledgment. We are grateful to Hideshi Okuda for his generous permission to use a light scattering instrument and his technical assistance and to Hiroko Kotani for her help with the gas chromatographic analysis. We also thank Akihito Abe for his help with a computer calculation.

Registry No. TTAB, 1119-97-7; TTAC, 4574-04-3; DDAC, 112-00-5; DDAB, 1119-94-4.

Characterization of Micellar Aggregates in Viscoelastic Surfactant Solutions. A Nuclear Magnetic Resonance and Light Scattering Study

Ulf Olsson,* Olle Söderman, and Paul Guéring[†]

Physical Chemistry 1, Chemical Center, University of Lund, S-221 00 Lund, Sweden
(Received: December 18, 1985; In Final Form: April 28, 1986)

An extensive proton nuclear magnetic resonance (^{1}H NMR) study of some two-component viscoelastic surfactant/water systems, viz. alkyltrimethylammonium salicylates and hexadecylpyridinium salicylate, is presented. Data from varying surfactant concentrations and temperatures as well as measurements showing the effect of added salt are given. The ^{1}H NMR bandshapes are analyzed with a model developed by Wennerström, which yields a correlation time for the slow motion(s) in such surfactant/water systems. The ^{1}H NMR bands start to broaden at concentrations just above the critical micelle concentrations. The broadening continues up to a concentration above which the bandshape remains constant as the concentration is further increased. These observations are discussed in terms of tumbling and flexibility of the surfactant aggregates. It is argued that coupling of lateral surfactant diffusion over the curved surface and segmental motions of the flexible surfactant aggregate can explain the constant bandshape. One key point in this conjecture is that there exists a very high degree of counterion association to the micellar aggregate, and this is confirmed with ^{1}H NMR self-diffusion measurements. Finally, some phase diagrams of the systems under study are presented, and by the combination of measurements of quasi-elastic and static light scattering, it is shown that the surfactant aggregates are rod shaped.

Introduction

Many single-chain ionic surfactants form roughly spherical micelles at a well-defined concentration, the critical micelle concentration, when dissolved in water. For some systems, the micelles retain the spherical shape up to very high concentrations, while in other systems, an aggregate growth is induced at higher surfactant concentrations. (For recent reviews on micellar formation, see ref 1 and 2.) For some micellar systems, it is possible to induce the aggregate growth at very low total surfactant concentrations. An example of this is hexadecyltrimethyl-

[†] Present address: Lab. de Spectroscopie Hertzienne de L'Ecole Normale, Supérieure, Paris, France.

(1) Wennerström, H.; Lindman, B. *Phys. Rep.* **1979**, *52*, 1.
(2) Lindman, B.; Wennerström, H. *Top. Curr. Chem.* **1980**, *87*, 1.

0022-3654/86/2090-5223$01.50/0